

PAPER • OPEN ACCESS

CHSH Bell tests for optical hybrid entanglement

To cite this article: Morteza Moradi *et al* 2024 *New J. Phys.* **26** 033019






View the [article online](#) for updates and enhancements.

You may also like

- [Generation of generalized hybrid entanglement in cavity electro–optic systems](#)
Feng-Yang Zhang and Chui-Ping Yang
- [Photonic schemes of distribution and reconstruction of an entangled state from hybrid entanglement between polarization and time-bin via quantum dot](#)
Jino Heo and Seong-Gon Choi
- [Hybrid Rabi interactions with traveling states of light](#)
Kimin Park, Julien Laurat and Radim Filip



PAPER

CHSH Bell tests for optical hybrid entanglementMorteza Moradi¹ , Juan Camilo López Carreño^{1,2}, Adam Buraczewski¹ , Thomas McDermott¹,
Beate Elisabeth Asenbeck³ , Julien Laurat³  and Magdalena Stobińska^{1,*} ¹ Institute of Informatics, Faculty of Mathematics, Informatics and Mechanics, University of Warsaw, Banacha 2, 02-097 Warsaw, Poland² Institute of Theoretical Physics, Faculty of Physics, University of Warsaw, Pasteura 5, 02-093 Warsaw, Poland³ Laboratoire Kastler Brossel, Sorbonne Université, CNRS, ENS-Université PSL, Collège de France, 4 Place Jussieu, 75005 Paris, France

* Author to whom any correspondence should be addressed.

E-mail: magdalena.stobinska@gmail.com**Keywords:** quantum information, Bell inequalities, entanglement testing, quantum optics, hybrid quantum entanglementSupplementary material for this article is available [online](#)

OPEN ACCESS

RECEIVED

9 November 2023

REVISED

14 February 2024

ACCEPTED FOR PUBLICATION

26 February 2024

PUBLISHED

15 March 2024

Original Content from
this work may be used
under the terms of the
[Creative Commons
Attribution 4.0 licence](#).Any further distribution
of this work must
maintain attribution to
the author(s) and the title
of the work, journal
citation and DOI.**Abstract**

Optical hybrid entanglement can be created between two qubits, one encoded in a single photon and another one in coherent states with opposite phases. It opens the path to a variety of quantum technologies, such as heterogeneous quantum networks, merging continuous- and discrete-variable encoding, and enabling the transport and interconversion of information. However, reliable characterization of the non-local nature of this quantum state is limited so far to full quantum state tomography. Here, we perform a thorough study of Clauser–Horne–Shimony–Holt Bell inequality tests, enabling practical verification of quantum nonlocality for optical hybrid entanglement. We show that a practical violation of this inequality is possible with simple photon number on/off measurements if detection efficiencies stay above 82%. Another approach, based on photon-number parity measurements, requires 94% efficiency but works well in the limit of higher photon populations. Both tests use no postselection of the measurement outcomes and they are free of the fair-sampling hypothesis. Our proposal paves the way to performing loophole-free tests using feasible experimental tasks such as coherent state interference and photon counting.

1. Introduction

Optical hybrid entanglement is a form of quantum correlations that embodies the original Schrödinger's *Gedankenexperiment* [1] by replacing the cat with a classical light beam, i.e. a single photon is entangled with a coherent light [2–5]. It may become a key asset in resource-efficient quantum computation [6], quantum key distribution [7–9], and quantum buses [10, 11]; it has already been employed in complex protocols which paved the way to building heterogeneous quantum network capabilities, e.g. entanglement swapping and a quantum-bit encoding converter [12, 13]. Furthermore, it was used to probe fundamental limits of quantum theory [14, 15], studying hybrid discrete- (DV) and continuous-variable (CV) quantum information [5, 16], and the information capacity of a photonic state [17].

Quantum technologies often require testing for quantum nonlocality in underlying resources. While these tests have been accomplished for two-mode CV states [18], this task becomes particularly challenging when dealing with optical hybrid entanglement. Its dual DV–CV nature implies that Bell nonlocality tests based on hybrid measurement strategies should be optimal. They involve a binary observable measured on the single photon mode and one with a continuous spectrum on the other mode. However, since implementing random Bell test settings in the photon number basis is not experimentally possible, strategies harnessing general qubit measurements are impractical. More universal approaches often employ coarse-graining of detection outcomes for multiphoton entanglement, which can impair Bell nonlocality tests [19, 20]. Moreover, hybrid quantum states decohere exponentially fast with the increasing photon

population of the classical light wave [16, 21, 22]. Therefore, how to design a nonlocality test for hybrid entanglement that can be set up in a laboratory, remains an open question.

Until now, nonlocality tests based on quantum steering inequality [23] and several strategies based on the Clauser–Horne–Shimony–Holt (CHSH) Bell inequality [24] have been outlined. In [25], the nonlocality of hybrid entanglement was tested with displaced parity measurements on both modes. A hybrid detection strategy was also discussed where the measurement on DV mode was replaced with a general qubit measurement. These tests need detection efficiencies of at least 90%. In [26], two hybrid strategies were considered, that involved either displaced parity or displaced on/off measurements. There, the minimal required detection efficiency is 83% for the former, and 63% for the latter test, respectively. However, performing a qubit rotation in the photon-number basis is currently challenging.

Other optical hybrid Bell nonlocality tests, e.g. hybrid polarization entanglement [27], can serve as a guideline. Although this state is physically different from the photon-number entanglement we consider, it shows mathematical similarities. The hybrid nonlocality testing strategies proposed for it involve displaced parity and displaced on/off measurements for the CV mode and a generalized polarization measurement for the DV mode. Albeit they can be implemented with polarizers and photon-number-resolving (PNR) detection of efficiencies higher than 82%, these Bell tests have not been performed yet.

Here, we perform a thorough analytical and numerical study of two practical CHSH Bell inequality tests possessing a high potential to achieve feasible verification of quantum nonlocality for the optical hybrid entanglement. They can be implemented in an experimental setup, where each mode interferes with a coherent field followed by on/off or parity measurements, realized by means of e.g. PNR detectors [28]. We show that the first test can achieve the inequality violation for detection efficiencies higher than 82% and amplitudes of the CV mode below 1.2. In the ideal, lossless conditions, this test would allow for a violation of up to 2.71. In contrast, the latter measurement scheme works with higher amplitudes but also sets higher requirements for system efficiencies, which must stay above 94%. This renders it less practical. Finally, for comparison, we also consider hybrid tests, modified for general qubit measurements, and show that in theory, this flavor of hybrid entanglement can maximally violate the CHSH Bell inequality. All the analyzed measurement schemes do not involve postselection and therefore, they have the capability to keep the detection loophole closed.

This paper is organized as follows. Section 2 briefly discusses the definition of optical hybrid entanglement state as considered in this study as well as its basic properties. In section 3 we introduce a general Bell test design based on the CHSH Bell inequality, including the experimental setup, model of losses used, and the theoretical background. Next, in section 4 we present and discuss numerical results obtained by applying various measurement schemes for the nonlocality tests. Section 5 is devoted to an outlook and conclusions.

2. Optical hybrid entanglement

Let us consider the following hybrid entanglement state that was recently generated [3] and subsequently used in various protocols [12, 13, 29, 30]

$$|\Psi\rangle = \frac{1}{\sqrt{2}} (|0\rangle_A |\text{cat}^-\rangle_B + |1\rangle_A |\text{cat}^+\rangle_B). \quad (1)$$

In mode A , a discrete-variable qubit is encoded in photon-number states $|0\rangle$ and $|1\rangle$ —the vacuum and single-photon Fock state, respectively. The qubit is entangled with mode B that carries two mutually orthogonal continuous-variable states, $|\text{cat}^-\rangle$ and $|\text{cat}^+\rangle$. Both of them are superpositions of coherent states of the same amplitude but opposite phases

$$|\text{cat}^\pm\rangle = \frac{1}{N_\pm} (|\gamma\rangle \pm |-\gamma\rangle), \quad (2)$$

where $N_\pm = \sqrt{2(1 \pm e^{-2|\gamma|^2})}$ is the normalization constant and $|\gamma\rangle = e^{-\frac{|\gamma|^2}{2}} \sum_{n=0}^{\infty} \frac{\gamma^n}{\sqrt{n!}} |n\rangle$ is a coherent state. States $|\text{cat}^\pm\rangle$ are orthogonal, $\langle \text{cat}^+ | \text{cat}^- \rangle = 0$, which stems from the fact that $|\text{cat}^+\rangle$ carries only even photon-number components while $|\text{cat}^-\rangle$ only odd ones. This property works as a hint that PNR-based measurement schemes could be the best suited for their discrimination.

Full characterization of $|\Psi\rangle$ was realized using efficient quantum state tomography [3] and quantum steering tests were also performed [23]. However, a full nonlocality test has not been carried out yet. Interestingly, in the limit of $\gamma \rightarrow 0$, $|\Psi\rangle$ tends to the single-photon entanglement $\frac{1}{\sqrt{2}} (|0\rangle|1\rangle - |1\rangle|0\rangle)$. Also in this case verification of nonlocality in $|\Psi\rangle$ is conceptually challenging and it has generated a lot of attention [31–36].

3. General Bell test design for optical hybrid entanglement

Verification of quantum nonlocality requires designing a viable Bell test. This task is quantum state-specific [37, 38] as universal methods for finding a well-matched one are not known. Moreover, experimental implementations of Bell tests are limited by the number of accessible measurement strategies, which in the case of photonic setups comprise polarization rotations, displacement operations, homodyne, and detectors of high efficiency, e.g. superconducting nanowires [39] or transition-edge sensors [40]. Furthermore, within the current state of the art, the implementation of rotations in the Fock state basis, which will result in the creation of superpositions of states with different photon numbers, is challenging.

The CHSH Bell inequality, which facilitated the first loophole-free Bell tests [41, 42], takes the form

$$S = \langle A_1 B_1 \rangle + \langle A_1 B_2 \rangle + \langle A_2 B_1 \rangle - \langle A_2 B_2 \rangle \leq 2, \quad (3)$$

where A_i (B_i), for $i = 1, 2$, are binary observables of values ± 1 , measured on mode A (B). It was successful because of its robustness against noise and errors in experimental settings. Quantum correlations allow S to achieve values up to $2\sqrt{2} \approx 2.83$ and subsequently violate inequality (3). Thus, observing CHSH values clearly crossing the classical boundary of 2 is the goal of any practical test.

We propose to employ the CHSH inequality and either on/off or parity measurements for testing the nonlocality in the optical hybrid entanglement state. In figure 1(a), two modes of the shared state $|\Psi\rangle$ are locally interfered with coherent fields, $|\alpha\rangle$ and $|\beta\rangle$, followed by measurements of efficiency $0 < \eta_{a,b} \leq 1$. The variable beam splitters' reflectivities r_a and r_b act as the Bell test settings. The registered readouts k and l are then coarse-grained into two sets, either zero/non-zero or even/odd numbers of photons (sections 4.1 and 4.2).

This design builds on a group theory result that maps two-mode Fock states $|n\rangle|\Sigma - n\rangle$ to Dicke spin- $\frac{\Sigma}{2}$ states with component $S_z = \frac{\Sigma}{2} - n$, by means of the Schwinger representation [43]. Next, we observe that any arbitrary rotation of S_z -spin component encoded in a product of Fock states is easily implemented using Fock state interference on a beam splitter [44]. Reflectivities set the spin rotation angles. We also note the fact that testing the nonlocality in photon-number correlations requires erasing 'how-many-photons' information before taking measurements. This step requires that we locally interfere each mode of the photon-number entangled state with a quantum superposition of indefinite number of photons, e.g. a coherent state, not merely with a Fock state. Effectively, if we examine this interference in the Fock state basis, it will amount not only to the spin rotation, but also to varying the spin value $\frac{\Sigma}{2}$ each time the measurements are taken. In this way, in the Bell test, we no longer need to perform rotations directly in the Fock state basis, but we carry out rotations of a spin that fluctuates in length instead. These Bell tests can detect nonlocality in a wide class of bipartite entanglement: squeezed vacuum, single-photon entanglement, entangled coherent states, and generalized Holland–Burnett states [25, 45–50].

In figure 1(b) we further modify the setup from figure 1(a) for generalized qubit measurements in mode A . The goal is to see how much improvement such a test can offer (sections 4.3 and 4.4). To this end, we assume that the above-mentioned rotations are experimentally feasible.

To investigate the collective effect of losses in the state generation, transmission, and imperfect detection in full optical tests, we model them with a beam splitter of transmittivity $\eta_{a,b}$ inserted in front of each detector. In hybrid Bell tests, we avoid the post-selection loophole by assigning the value $+1$ to the measurement outcome of observable A_i if a 'no-detection' event in mode A occurs, i.e. the effective observable could be written as $A_i^{\text{eff}} = \eta A_i + (1 - \eta)\mathbb{1}$, where $\mathbb{1}$ denotes the identity operator.

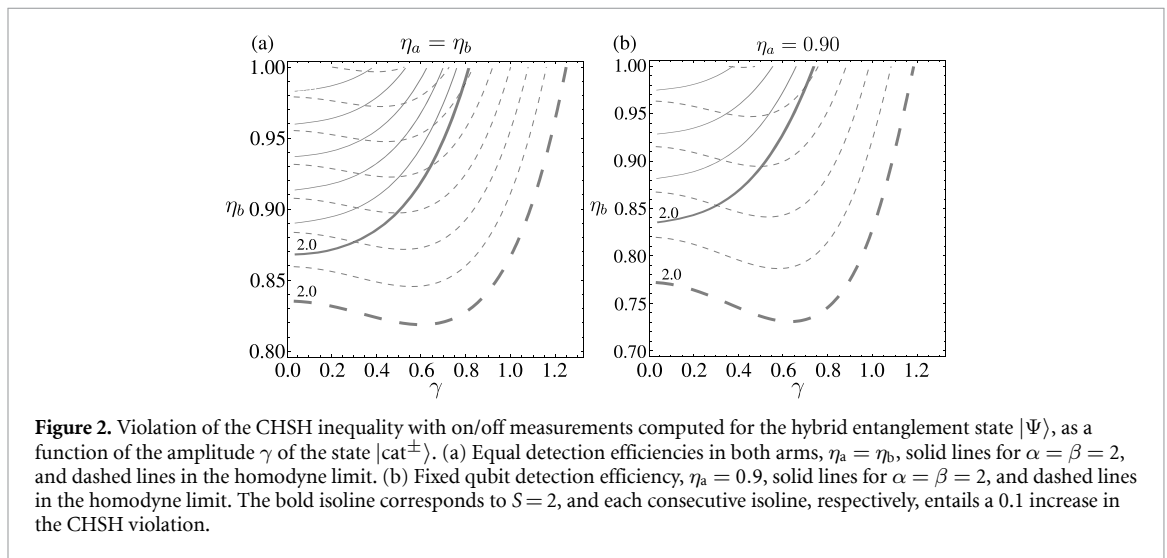
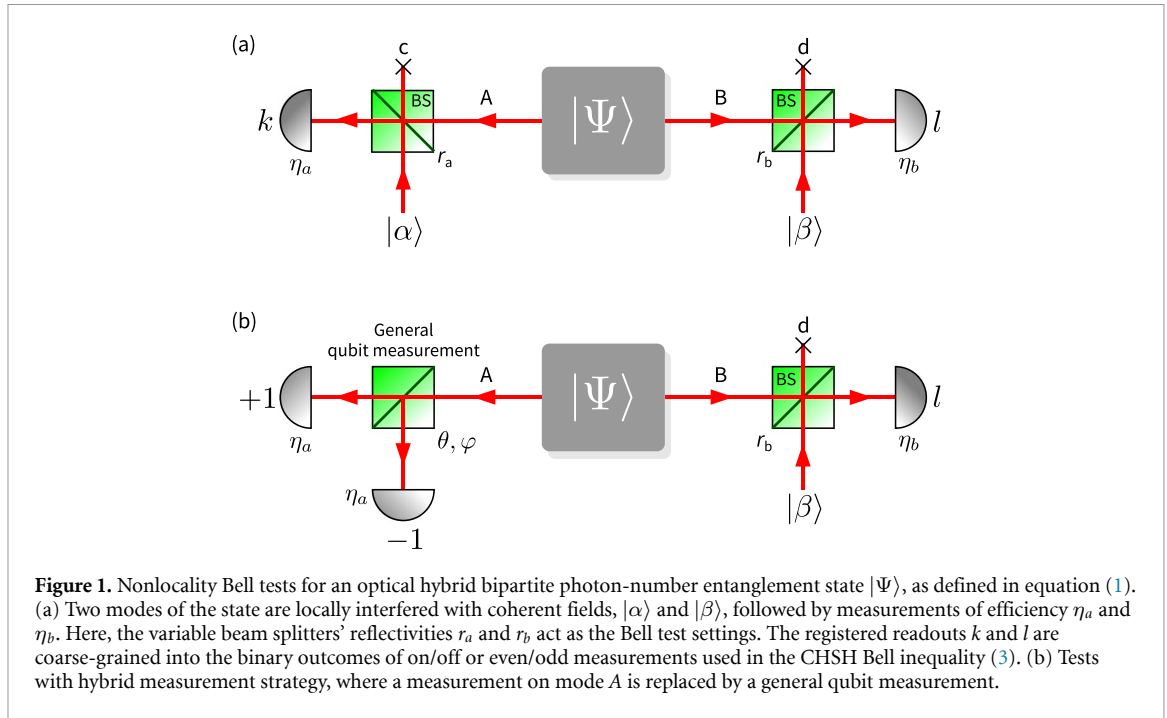
We also notice that for the homodyne limit (HD), characterized by very small reflectivities, $r_a, r_b \rightarrow 0$, and large amplitudes of the coherent fields, $|\alpha|^2, |\beta|^2 \rightarrow \infty$, the beam splitter interference may be approximated with displacement operators $D(\delta_{\alpha,\beta})$ with $\delta_\alpha = -i\alpha\sqrt{r_a}$ and $\delta_\beta = -i\beta\sqrt{r_b}$ [51, 52]. In this case, these displacements become the measurement settings. However, in this limit, the photon population of the local oscillators is several orders of magnitude larger than that of the measured state, $|\alpha|^2, |\beta|^2 \gg |\gamma|^2$, which may pose additional experimental challenges, e.g. the PNR detection of large photon numbers [51, 53].

Details of analytical derivations and numerical methods used for obtaining the results are presented in sections 4.1–4.4 are given in the supplementary material.

4. Results

4.1. CHSH test with on/off measurements

The first CHSH Bell test that we will outline is based on the scheme shown in figure 1(a), where the detection outcomes k and l are split into four sets according to the vacuum and non-vacuum events registered in



modes A and B , $\{(k=0, l=0), (k=0, l \neq 0), (k \neq 0, l=0), (k \neq 0, l \neq 0)\}$; they correspond to the binary measurement outcomes $\{(+1, +1), (+1, -1), (-1, +1), (-1, -1)\}$ assigned to A and B , respectively. The on/off measurement operator takes the form

$$\Pi_{\text{on/off}} = |0\rangle\langle 0| - \sum_{n=1}^{\infty} |n\rangle\langle n| = 2|0\rangle\langle 0| - 1. \tag{4}$$

We would like to emphasize that $\Pi_{\text{on/off}}$ describes solely the detection, not the observable employed in the Bell test. It is challenging to concisely analytically express a single observable A_i (or B_j) and to reveal its dependence on the settings of the Bell test (r_a and r_b), but we can write down explicitly the correlation function between these observables as follows

$$\langle A_i B_j \rangle = \text{Tr} \left\{ \Pi_{\text{on/off}}^{(A)} \Pi_{\text{on/off}}^{(B)} \text{Tr}_{c,d} \left[\mathcal{U}_{\text{BS}}(r_a) \mathcal{U}_{\text{BS}}(r_b) \rho_{\Psi} \rho_{\alpha} \rho_{\beta} \mathcal{U}_{\text{BS}}^{\dagger}(r_b) \mathcal{U}_{\text{BS}}^{\dagger}(r_a) \right] \Pi_{\text{on/off}}^{(B)\dagger} \Pi_{\text{on/off}}^{(A)\dagger} \right\}, \tag{5}$$

where $\rho_{\Psi} = |\Psi\rangle\langle\Psi|$, ρ_{α} and ρ_{β} are the coherent states $|\alpha\rangle$ and $|\beta\rangle$. The action of a beam splitter is described by the unitary $\mathcal{U}_{\text{BS}}(r) = e^{-i\mu(a^{\dagger}b - ab^{\dagger})}$, where $\mu = 2 \arcsin \sqrt{r}$, r is the beam splitter reflectivity and a, b denote the annihilation operators of interfering modes.

To compute the maximal value of parameter S and achieve the CHSH inequality violation for given γ and detection efficiencies $\eta_{a,b}$, we numerically optimize equation (3) with the correlation functions given by equation (5), with respect to the Bell test settings $r_{a_{1,2}}, r_{b_{1,2}}$ for given parameters α, β . Next, we optimize the amplitudes α, β to obtain the minimal detection efficiencies $\eta_{a,b}$ required for the violation. Numerical optimization is simplified by using the real domain for parameters γ, α and β . This approach is viable as phases can be aligned in the experimental implementation.

The results for the on/off measurements are depicted in figure 2. In panel (a) we set equal detection efficiencies $\eta_a = \eta_b$ and fix the parameters $\alpha = \beta = 2$ for solid lines. In the limit $\gamma \rightarrow 0$ and perfect detection ($\eta_{a,b} = 1$) we obtain $S = 2.57$. The value of S gradually drops for higher γ and reaches the boundary $S = 2$ for $\gamma = 0.8$, because the odds of spotting the zero-photon measurement quickly vanishes for highly-occupied states. Observing Bell inequality violation becomes also impossible below $\eta_a = \eta_b = 0.87$. For comparison, when we set higher $\alpha = \beta = 10$, in the limit $\gamma \rightarrow 0$ and perfect detection we obtain maximum violation of $S = 2.68$.

The computation results for the homodyne limit are shown by the dashed lines in figure 2(a). We first derived an analytical formula for correlation functions and then numerically maximized the S with respect to the Bell test settings $\delta_{\alpha_{1,2}}, \delta_{\beta_{1,2}}$. We found that in this case, the CHSH violation is higher than the solid lines, and it is also observed for a wider span of γ . Furthermore, the maximum value of the violation increases to $S = 2.71$ for $\gamma = 0.4$ and for the settings $\delta_{\alpha_1} = 0.18, \delta_{\alpha_2} = -0.56, \delta_{\beta_1} = 0.17, \delta_{\beta_2} = -0.61$, and the minimum efficiency that still provides violation is $\eta_{a,b} = 0.82$ for $\gamma = 0.6$.

Next, we studied the interplay between the minimal requirements for unequal detection efficiencies. The solid lines in figure 2(b) show the violations achieved for fixed qubit detection efficiency, $\eta_a = 0.9$ and $\alpha = \beta = 2$. They are observed for $\gamma < 0.75$ and $\eta_b > 0.83$. This gain comes at the expense of lowering the value of maximal violation to $S = 2.35$.

The dashed lines in figure 2(b) display the CHSH violation for $\eta_a = 0.9$ in the homodyne limit. Here, the maximal achieved value is higher than solid lines, reaching $S = 2.5$ for $\gamma = 0.42$, and the minimal efficiency that still provides violation gets to $\eta_b = 0.73$ for $\gamma = 0.63$.

In summary, our results show that significant CHSH violations can be achieved for hybrid entanglement state when performing on/off measurements. Notably, such violations can be reached even when the intensity of the local coherent state is comparable to the photonic occupation of the state under study. We also calculated how S increases in the homodyne limit and showed that we can reach a higher violation in this limit.

4.2. CHSH test with parity measurements

Let us now perform coarse-graining of the measurement results from figure 1(a) by assigning +1 to the detection of even numbers of photons ($k = \text{even}$ or $l = \text{even}$), and -1 to the detection of odd numbers of photons ($k = \text{odd}$ or $l = \text{odd}$). This strategy mimics the use of parity measurements on modes A and B with

$$\Pi_{\text{parity}} = \sum_{n=0}^{\infty} (-1)^n |n\rangle\langle n|. \quad (6)$$

Following the steps described in section 4.1, we numerically optimize the CHSH value S in equation (3) with correlations computed using equation (5) but replacing the operator $\Pi_{\text{on/off}}$ with Π_{parity} from equation (6).

The results for the parity measurement are shown in figure 3. Panel (a) depicts computations for equal efficiencies $\eta_a = \eta_b$. Here the $\alpha = \beta = 1$ case is shown by the solid lines and provides us with the minimum $\eta_{a,b} = 0.96$ for which we see the violation. We find that the maximal CHSH value increases from $S = 2.17$ for $\gamma \rightarrow 0$ to $S = 2.24$ for $\gamma = 2$. We note that these measurements allow us to observe violation for larger amplitudes of γ than with on/off measurements. In fact, with this measurement, one could get $S > 2$ for $\eta \rightarrow 1$ independently of γ , unlike for the on/off case, where γ was limited. However, parity measurements, in general, require higher detection efficiencies, because losing a photon can turn an even number of photons into an odd one, and vice versa. The results corresponding to the homodyne limit are represented by dashed lines. In this case, the violation of $S = 2.39$ is achieved for $\gamma = 2$ and it will increase to maximum violation of $S = 2.44$ for $\gamma \rightarrow \infty$. However, it very quickly degrades with losses. The lowest efficiency for which $S > 2$ is $\eta_{a,b} = 0.94$ for $\gamma = 0.54$.

Figure 3(b) shows computations for $\eta_a = 0.95$, which is almost the minimum required efficiency for achieving CHSH violation. Here, the solid lines correspond to $\alpha = \beta = 1$, and $S = 2.14$ is reached for $\gamma = 2$. A value of η_b required to witness any violation is $\eta_b = 0.96$ for $\gamma = 0.5$. In the homodyne limit (dashed lines), the violation of $S = 2.29$ is attained for $\gamma = 2$ which increased to $S = 2.34$ for $\gamma \rightarrow \infty$, and $S > 2$ is reached for minimum $\eta_b = 0.93$ at $\gamma = 0.5$.

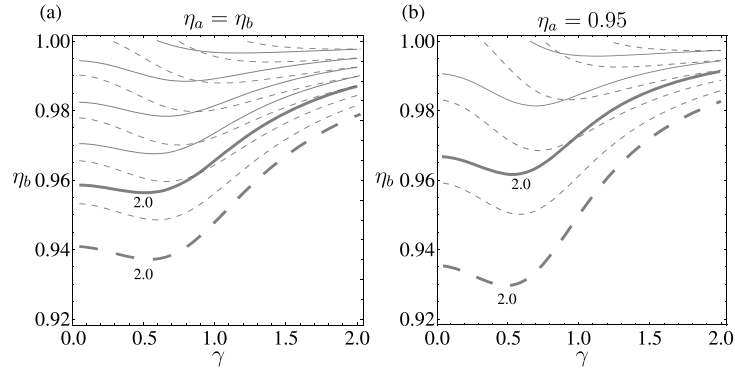


Figure 3. Violation of the CHSH inequality with parity measurements computed for the hybrid entanglement state $|\Psi\rangle$, as a function of the amplitude γ of the state $|\text{cat}^\pm\rangle$. (a) Equal detection efficiencies in both arms, $\eta_a = \eta_b$, solid lines for $\alpha = \beta = 1$, and dashed lines in the homodyne limit. (b) Fixed qubit detection efficiency, $\eta_a = 0.95$, solid lines for $\alpha = \beta = 1$, and dashed lines in the homodyne limit. The bold isoline corresponds to $S = 2$, and each consecutive isoline, respectively, entails a 0.05 increase in the CHSH violation.

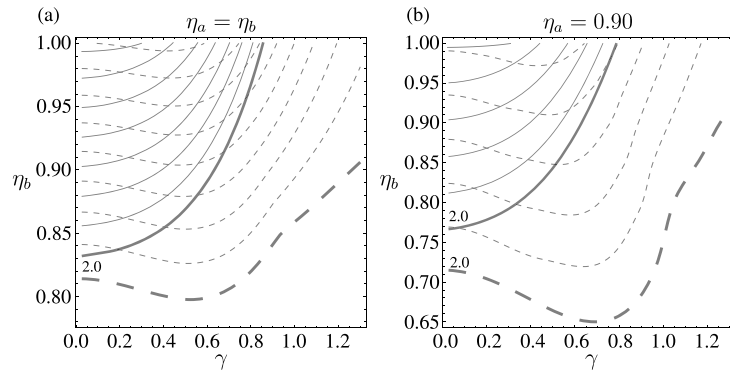


Figure 4. Violation of the hybrid CHSH Bell test with on/off hybrid measurements computed for the hybrid entanglement state $|\Psi\rangle$, as a function of the amplitude γ of the state $|\text{cat}^\pm\rangle$. (a) Equal detection efficiencies in both arms, $\eta_a = \eta_b$, solid lines for $\alpha = \beta = 2$, and dashed lines in the homodyne limit. (b) Fixed qubit detection efficiency, $\eta_a = 0.90$, solid lines for $\alpha = \beta = 2$, and dashed lines in the homodyne limit. The bold isoline corresponds to $S = 2$, and each consecutive isoline, respectively, entails a 0.1 increase in the CHSH violation.

Our results show that CHSH violations can also be achieved for hybrid entanglement state when performing parity measurements. The magnitudes of the violations are lower than in the on/off case, and require better detection efficiencies, but can be observed at larger values of the amplitude γ . In both cases, the ideal setting which gave us the maximum violation happens in the homodyne limit.

4.3. Hybrid CHSH test with on/off measurements

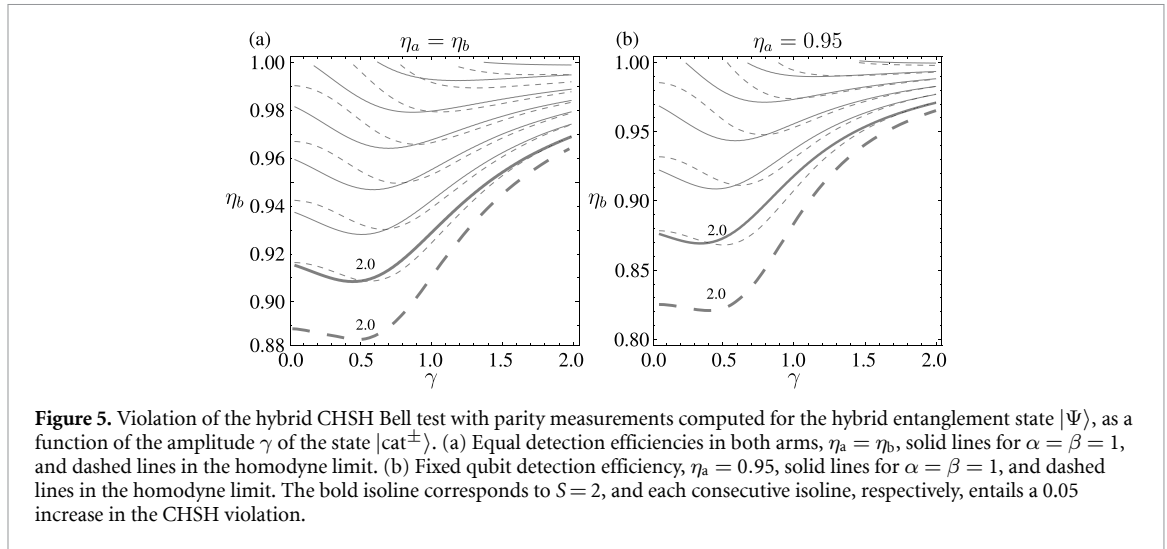
Another strategy linked to the specific nature of the considered state is to perform the hybrid Bell test shown in figure 1(b). In this design, a general qubit measurement is performed on the single-photon subsystem, while on/off measurements, equation (4), are applied to mode B . Every qubit observable can be described in terms of Pauli operators σ_X , σ_Y , and σ_Z [54]

$$A_j = \sin\theta_j \cos\phi_j \sigma_X + \sin\theta_j \sin\phi_j \sigma_Y + \cos\theta_j \sigma_Z, \quad (7)$$

where $j = 1, 2$ correspond to two measurement settings used in mode A in the test.

We follow the steps described in section 4.1 for the optimization of the CHSH value with the on/off measurements, but we apply the observable defined equation (7) in mode A . The results, depicted by solid lines in figure 4(a), are computed for $\alpha = \beta = 2$ and $\eta_a = \eta_b$. Here, $S = 2.72$ is achieved for $\gamma \rightarrow 0$, but CHSH violation is reached only for $\eta_{a,b} \geq 0.82$. The range for which the violation can be observed is bounded by $\gamma = 0.88$. Solid lines in figure 4(b) display $\eta_a = 0.9$ for $\alpha = \beta = 2$, for which the maximal violation is $S = 2.54$ but the minimal efficiency needed for the violation drops to $\eta_b = 0.77$.

In the homodyne limit, the minimal required detection efficiency to observe any CHSH inequality violation is $\eta_{a,b} = 0.8$, shown by dashed lines in figure 4(a). The highest violation of $S = 2\sqrt{2} \approx 2.83$ is



obtained for $\gamma = \sqrt{\ln 2}/2 \approx 0.42$. For $\eta_a = 0.9$, dashed lines in figure 4(b), the minimal η_b equals 0.65 and the maximal violation is $S = 2.55$.

The maximal violation, depicted with the dashed lines in figure 4(a), can be additionally shown analytically using the CHSH rigidity theorem. This theorem states that if a quantum state maximally violates the CHSH inequality, it is equivalent to the maximally entangled Bell pair $\frac{1}{\sqrt{2}}(|0\rangle|0\rangle + |1\rangle|1\rangle)$, while the measurements used are equivalent to the canonical qubit measurements $A_1 = \sigma_Z$, $A_2 = \sigma_X$, $B_1 = \frac{1}{\sqrt{2}}(\sigma_Z + \sigma_X)$, $B_2 = \frac{1}{\sqrt{2}}(\sigma_Z - \sigma_X)$ [55, 56]. This prerequisite is fulfilled by $|\Psi\rangle$, because equation (1) already possesses the form of a Bell pair. Orthonormal states $|e_0\rangle = |\text{cat}^- \rangle$ and $|e_1\rangle = |\text{cat}^+ \rangle$ can be considered as two states of a multiphoton qubit, but they must be complemented by an arbitrary set of orthonormal $|e_i\rangle$ where $i \geq 2$ to form the full basis in an infinite-dimensional Hilbert space.

In order to analytically investigate this theorem, let us take $A_1 = \sigma_Z$ and $A_2 = \sigma_X$, as well as $\delta_{\beta_{1,2}} = \pm\gamma$. With regards to the measurement operators acting on mode B , we note that in the homodyne limit they can be expressed as $B_j = D(\delta_{\beta_j})\Pi_{\text{on/off}}D^\dagger(\delta_{\beta_j}) = 2|\delta_{\beta_j}\rangle\langle\delta_{\beta_j}| - \mathbb{1}$, $j = 1, 2$. In the basis $|e_i\rangle$, they have the following form

$$B_j = \tilde{B}_j \oplus -\mathbb{1}, \quad (8a)$$

$$\tilde{B}_j = (-1)^{j-1} \sqrt{1 - e^{-4\gamma^2}} \sigma_X + e^{-2\gamma^2} \sigma_Z, \quad (8b)$$

where $j = 1, 2$. The supplementary material details the full proof.

Now, when we substitute $\gamma = \frac{1}{2}\sqrt{\ln 2} \approx 0.42$, then $B_1 = \frac{1}{\sqrt{2}}(\sigma_Z + \sigma_X)$ and $B_2 = \frac{1}{\sqrt{2}}(\sigma_Z - \sigma_X)$ and the maximal violation of the CHSH inequality $S = 2\sqrt{2}$ can be observed, thus proving the CHSH rigidity for the optical hybrid entanglement. This stays in agreement with [57].

In summary, the hybrid Bell test, in which a general qubit measurement is performed on mode A while mode B is tested with on/off measurements, allows one to achieve higher CHSH inequality violations compared to the case where on/off measurements are performed on both modes. Furthermore, in the homodyne limit, this approach allows one to observe the maximal CHSH violation of $2\sqrt{2}$ for the hybrid entanglement, showing that this state is equivalent to the maximally entangled Bell pair.

4.4. Hybrid CHSH test with parity measurements

Lastly, we consider a hybrid test in which general qubit measurements, equation (7), are performed on mode A , and the parity measurements, equation (6), on mode B . Numerical computations follow the steps from section 4.3.

The results, displayed with solid lines in figure 5(a), are computed for $\alpha = \beta = 1$ and $\eta_a = \eta_b$. Here, the maximum violation reaches $S = 2.62$ for $\gamma = 2$ and drops to $S = 2$ for $\eta_{a,b} = 0.91$ and $\gamma = 0.6$. In the case of $\eta_b = 0.95$, computed for $\alpha = \beta = 1$ (solid lines in panel (b)), the maximal violation of $S = 2.52$ is reached for $\gamma = 2$. The CHSH inequality is minimally violated for $\eta_b = 0.87$ for $\gamma = 0.45$.

In the homodyne limit, the CHSH parameter computed for $\eta_a = \eta_b$ reaches $S = 2.77$ for $\gamma = 2$, shown by dashed lines in panel (a). The minimum required efficiency is $\eta_a = \eta_b > 0.88$ for $\gamma = 0.47$. For $\eta_a = 0.95$,

dashed lines in panel (b), minimal required $\eta_b > 0.82$ for $\gamma = 0.37$, while S takes the maximal value of 2.69 for $\gamma \rightarrow \infty$. The CHSH inequality in this case also is maximally violated for $\gamma \rightarrow \infty$ and $\eta_{a,b} \rightarrow 1$, which can be proved analytically. In this limit, $\langle -\gamma|\gamma \rangle = 0$ and observables B_1 and B_2 become

$$B_j = e^{-2|\delta_j|^2} (\cos \varphi_j \sigma_Z - \sin \varphi_j \sigma_Y), \quad (9)$$

where $\varphi_j = 4\gamma \text{Im}(\delta_j)$ and $j = 1, 2$. Then, by substituting $\delta_{\beta_{1,2}} = \pm i\pi/16\gamma$ one gets $B_1 = \frac{1}{\sqrt{2}}(\sigma_Z - \sigma_Y)$ and $B_2 = \frac{1}{\sqrt{2}}(\sigma_Z + \sigma_Y)$, which are the canonical measurements up to a rotation in the X–Y plane. The CHSH inequality can be maximally violated, $S = 2\sqrt{2}$, for $A_1 = \sigma_Z, A_2 = \sigma_Y$.

To sum up this case, in analogy to section 4.3, the hybrid CHSH test with parity measurements allows one to achieve higher CHSH Bell inequality violations than the test using parity measurements in both modes, at the expense of the feasibility of the experimental scheme. It also allows one to obtain the maximal violation for a specific set of system parameters.

5. Discussion and conclusion

We have demonstrated that the nonlocality in an optical hybrid entanglement state can be experimentally confirmed by violating the CHSH Bell inequality. In the test, each mode of $|\Psi\rangle$, equation (1), interferes with a local coherent state $|\alpha\rangle$ and $|\beta\rangle$, respectively, on variable beam splitters of reflectivities r_a and r_b , and subsequently measured. While $r_{a,b}$ act as the Bell test settings, splitting the detection outcomes into two sets of zero and non-zero or even/odd numbers of photons allows us to realize binary measurements. This test requires small fine-tuned beam splitter reflectivities. Although the proposed test is challenging to implement due to inevitable losses in the optical paths and imperfect detection, it is within reach of current detection technology. There is a strong ongoing effort to develop highly efficient photon number resolution with superconducting-nanowire detectors or transition-edge sensors [39, 40, 58–67]. Indeed, efficiencies up to 98% with a photon-resolving power of up to 7 photons were reported for transition-edge-sensors (TES) [58]. This puts a limit on the combinations of γ, α, β , and r that can be used in the current proposal and indeed cover most of the cases highlighted in figures 2 and 3.

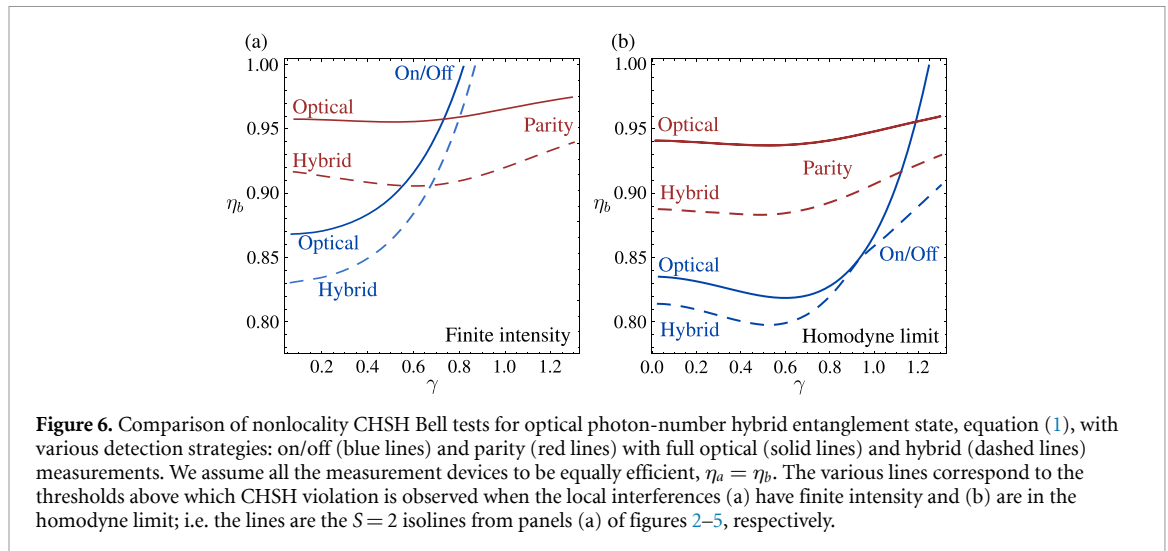
For the non-homodyne limit with $\alpha = \beta = 2$ our result is depicted by solid lines in figure 2. Here, significant CHSH Bell inequality violations, up to $S = 2.57$, are demonstrated for hybrid entangled state $|\Psi\rangle$ with amplitudes $\gamma < 0.81$, and on/off measurements with detection efficiencies above 0.87. By increasing the value of α, β the optimal Bell value also increases.

Our main result is shown by dashed lines in figure 2, computed for the same on/off measurement but this time in the homodyne limit, i.e. $r_{a,b} \rightarrow 0$ and $\alpha, \beta \rightarrow \infty$, where the local interferences of $|\Psi\rangle$ with coherent states amount to displacement operations [52]. Here we observe Bell violations, up to $S = 2.71$ in ideal circumstances, which are demonstrated for states with amplitudes $\gamma < 1.25$, and on/off measurements with detection efficiencies above 0.82. For example for $\gamma = 0.44$ and efficiencies $\eta_{a,b} \geq 0.95$, it gave the Bell violation of $S = 2.51$.

In figure 3 we present the result for parity measurement. In the ideal lossless conditions, this allows one to perform the even/odd Bell test for arbitrarily large amplitude γ , reaching the maximal value of $S = 2.44$. However, this measurement is quickly spoiled by losses that remove photons from the state and so these violations are very fragile and vanish quickly by experimental imperfections, e.g. when detection efficiencies drop below 0.96 for $\alpha = \beta = 1$. We note that current PNR capabilities will also be a limiting factor in the case of the homodyne limit.

The results presented in figures 4 and 5 are interesting for studying the nonlocality in the hybrid entanglement state. We enhanced our two measurement strategies with a general qubit measurement performed in the single-photon subsystem. This allowed us to maximally violate the CHSH inequality, up to $S = 2\sqrt{2}$. For example, it lets us decrease the required minimal efficiency of the measurement in the on/off test to $\eta_{a,b} \geq 0.8$ and in the parity test to $\eta_{a,b} > 0.88$. An interesting observation in this context is that when employing the photon counting Bell test on the maximally entangled states in (1), CHSH violation can be achieved even when the efficiency is below the Eberhard limit [68] (i.e. for $\eta < 2\sqrt{2} - 2 \approx 0.83$). This is because, in contrast to conventional Bell tests, the losses of photons are considered as an output in our Bell test scenario which makes it more robust to the losses.

Our numerical computations are summarised in figure 6, where we show a comparison of the thresholds above which CHSH violation occurs, as a function of both the detection efficiency, as well as the amplitude γ . Panel (a) displays the lines obtained when the local interference is done with a coherent state with finite intensity, while in panel (b) we show the counterpart in the homodyne limit. In both cases, we find that on/off measurements are more robust to imperfect detection and transmission losses, while parity measurements allow violations for higher values of γ . Moreover, regardless of the type of measurement, the



hybrid strategies provide a clear enhancement of the results, lowering the efficiency required to observe CHSH violations. The Supplemental Material includes a table with all the detailed results of the computations.

Our results give interesting insights from both fundamental and technological standpoints. They show ways to study the quantum nonlocality of optical hybrid entangled states, as well as of more general complex bipartite entanglement merging the CV and DV realms.

Data availability statement

All data that support the findings of this study are included within the article (and any supplementary files).

Acknowledgments

M M, A B, T M and M S were supported by the European Union’s Horizon 2020 research and innovation programme under the Marie Skłodowska-Curie project ‘AppQInfo’ No. 956071. M S and A B were supported by the National Science Centre ‘Sonata Bis’ Project No. 2019/34/E/ST2/00273, the QuantERA II Programme that has received funding from the European Union’s Horizon 2020 research and innovation programme under Grant Agreement No. 101017733, Project ‘PhoMemtor’ No. 2021/03/Y/ST2/00177. M S, A B and T M were supported by the Foundation for Polish Science ‘First Team’ Project No. POIR.04.04.00-00-220E/16-00 (originally FIRST TEAM/2016-2/17). J C L C was supported by the Polish National Agency for Academic Exchange (NAWA) under project TULIP with number PPN/U LM/2020/1/00235 and from the Polish National Science Center (NCN) ‘Sonatina’ project CAMEL with number 2021/40/C/ST2/00155. J L is a member of the Institut Universitaire de France. This work was supported by the ANR in the framework of France 2030 (ANR-22-PETQ-0011) and via ShoQC project (19-QUAN-0005-05). We gratefully acknowledge Poland’s high-performance computing infrastructure PLGrid (HPC Centers: ACK Cyfronet AGH) for providing computer facilities and support within computational Grant No. PLG/2023/016211. We thank A Mikos-Nuszkiewicz for discussions.

ORCID iDs

Morteza Moradi  <https://orcid.org/0000-0001-7971-7335>
 Adam Buraczewski  <https://orcid.org/0000-0002-8742-3844>
 Beate Elisabeth Asenbeck  <https://orcid.org/0000-0003-0614-3697>
 Julien Laurat  <https://orcid.org/0000-0001-8318-6514>
 Magdalena Stobińska  <https://orcid.org/0000-0002-5168-433X>

References

- [1] Schrödinger E 1935 Die gegenwärtige situation in der quantenmechanik *Naturwissenschaften* **23** 844
- [2] Jeong H, Zavatta A, Kang M, Lee S-W, Costanzo L S, Grandi S, Ralph T C and Bellini M 2014 Generation of hybrid entanglement of light *Nat. Photon.* **8** 564–9

- [3] Morin O, Huang K, Liu J, Le Jeannic H, Fabre C and Laurat J 2014 Remote creation of hybrid entanglement between particle-like and wave-like optical qubits *Nat. Photon.* **8** 570–4
- [4] Huang K, Le Jeannic H, Morin O, Darras T, Guccione G, Cavaillès A and Laurat J 2019 Engineering optical hybrid entanglement between discrete-and continuous-variable states *New J. Phys.* **21** 083033
- [5] Andersen U L, Neergaard-Nielsen J S, van Loock P and Furusawa A 2015 Hybrid discrete-and continuous-variable quantum information *Nat. Phys.* **11** 713
- [6] Lee S-W and Jeong H 2013 Near-deterministic quantum teleportation and resource-efficient quantum computation using linear optics and hybrid qubits *Phys. Rev. A* **87** 022326
- [7] Rigas J, Gühne O and Lütkenhaus N 2006 Entanglement verification for quantum-key-distribution systems with an underlying bipartite qubit-mode structure *Phys. Rev. A* **73** 012341
- [8] Wittmann C, Fürst J, Wiechers C, Elser D, Häseler H, Lütkenhaus N and Leuchs G 2010 Witnessing effective entanglement over a 2 km fiber channel *Opt. Express* **18** 4499
- [9] Yin H-L and Chen Z-B 2019 Coherent-state-based twin-field quantum key distribution *Sci. Rep.* **9** 14918
- [10] Spiller T P, Nemoto K, Braunstein S L, Munro W J, van Loock P and Milburn G J 2006 Quantum computation by communication *New J. Phys.* **8** 30
- [11] van Loock P, Munro W J, Nemoto K, Spiller T P, Ladd T D, Braunstein S L and Milburn G J 2008 Hybrid quantum computation in quantum optics *Phys. Rev. A* **78** 022303
- [12] Guccione G, Darras T, Le Jeannic H, Verma V B, Nam S W, Cavaillès A and Laurat J 2020 Connecting heterogeneous quantum networks by hybrid entanglement swapping *Sci. Adv.* **6** eaba4508
- [13] Darras T, Asenbeck B E, Guccione G, Cavaillès A, Le Jeannic H and Laurat J 2023 A quantum-bit encoding converter *Nat. Photon.* **17** 165–70
- [14] Chen Y 2013 Macroscopic quantum mechanics: theory and experimental concepts of optomechanics *J. Phys. B: At. Mol. Opt. Phys.* **46** 104001
- [15] Aspelmeyer M, Kippenberg T J and Marquardt F 2014 Cavity optomechanics *Rev. Mod. Phys.* **86** 1391
- [16] van Loock P 2011 Optical hybrid approaches to quantum information *Laser Photon. Rev.* **5** 167
- [17] Nape I, Ndagano B, Perez-Garcia B, Hernandez-Aranda R I, Roux F S, Konrad T and Forbes A 2017 Hybrid entanglement for quantum information and communication applications *Proc. SPIE 10347, Optical Trapping and Optical Micromanipulation XIV* vol 1034711
- [18] Chen Z-B, Pan J-W, Hou G and Zhang Y-D 2002 Maximal violation of Bell's inequalities for continuous variable systems *Phys. Rev. Lett.* **88** 040406
- [19] Stobińska M, Sekatski P, Buraczewski A, Gisin N and Leuchs G 2011 Bell-inequality tests with macroscopic entangled states of light *Phys. Rev. A* **84** 034104
- [20] Stobińska M, Töppel F, Sekatski P and Buraczewski A 2014 Towards loophole-free Bell inequality test with preselected unsymmetrical singlet states of light *Phys. Rev. A* **89** 022119
- [21] Zurek W H 2003 Decoherence einselection and the quantum origins of the classical *Rev. Mod. Phys.* **75** 715
- [22] Le Jeannic J, Cavaillès A, Huang K, Filip R and Laurat J 2018 Slowing quantum decoherence by squeezing in phase space *Phys. Rev. Lett.* **120** 073603
- [23] Cavaillès A, Le Jeannic H, Raskop J, Guccione G, Markham D, Diamanti E, Shaw M D, Verma V B, Nam S W and Laurat J 2018 Demonstration of Einstein–Podolsky–Rosen steering using hybrid continuous- and discrete-variable entanglement of light *Phys. Rev. Lett.* **121** 170403
- [24] Clauser J F, Horne M A, Shimony A and Holt R A 1969 Proposed experiment to test local hidden-variable theories *Phys. Rev. Lett.* **23** 880
- [25] Ketterer A 2016 Modular variables in quantum information *PhD Thesis* Université Paris 7, Sorbonne Paris Cité
- [26] Cavaillès A 2019 Non-locality tests and quantum communication protocols using hybrid entanglement of light *PhD Thesis* Sorbonne Université
- [27] Kwon H and Jeong H 2013 Violation of the Bell–Clauser–Horne–Shimony–Holt inequality using imperfect photodetectors with optical hybrid states *Phys. Rev. A* **88** 052127
- [28] Gerrits T et al 2011 On-chip, photon-number-resolving, telecommunication-band detectors for scalable photonic information processing *Phys. Rev. A* **84** 060301
- [29] Le Jeannic H, Cavaillès A, Raskop J, Huang K and Laurat J 2018 Remote preparation of continuous-variable qubits using loss-tolerant hybrid entanglement of light *Optica* **5** 1012–5
- [30] Parker R C, Joo J and Spiller T P 2020 Photonic hybrid state entanglement swapping using cat state superpositions *Proc. R. Soc. A* **476** 2243
- [31] Tan S M, Walls D F and Collett M J 1991 Nonlocality of a single photon *Phys. Rev. Lett.* **66** 252
- [32] Cooper J J and Dunningham J A 2008 Single particle nonlocality with completely independent reference states *New J. Phys.* **10** 113024
- [33] Das T, Karczewski M, Mandarino A, Markiewicz M, Woloncewicz B and Żukowski M 2021 Can single photon excitation of two spatially separated modes lead to a violation of Bell inequality via weak-field homodyne measurements? *New J. Phys.* **23** 073042
- [34] Das T, Karczewski M, Mandarino A, Markiewicz M, Woloncewicz B and Żukowski M 2022 Remarks about Bell-nonclassicality of a single photon *Phys. Lett. A* **435** 128031
- [35] Das T, Karczewski M, Mandarino A, Markiewicz M, Woloncewicz M B and Żukowski M 2022 Comment on ‘Single particle nonlocality with completely independent reference states’ *New J. Phys.* **24** 038001
- [36] Das T, Karczewski M, Mandarino A, Markiewicz M and Żukowski M 2022 Optimal interferometry for bell nonclassicality induced by a vacuum-one-photon qubit *Phys. Rev. Appl.* **18** 034074
- [37] Horodecki R, Horodecki P, Horodecki M and Horodecki K 2009 Quantum entanglement *Rev. Mod. Phys.* **81** 865
- [38] Brunner N, Cavalcanti D, Pironio S, Scarani V and Wehner S 2014 Bell nonlocality *Rev. Mod. Phys.* **86** 419
- [39] Reddy D V, Nerem R R, Nam S W, Mirin R P and Verma V B 2020 Superconducting nanowire single-photon detectors with 98% system detection efficiency at 1550 nm *Optica* **7** 1649
- [40] Lita A E, Miller A J and Nam S W 2008 Counting near-infrared single-photons with 95% efficiency *Opt. Express* **16** 3032
- [41] Giustina M et al 2013 Bell violation using entangled photons without the fair-sampling assumption *Nature* **497** 227
- [42] Giustina M et al 2015 Significant-loophole-free test of Bell's theorem with entangled photons *Phys. Rev. Lett.* **115** 250401
- [43] Chruściński D and Jamiołkowski A 2004 *Geometric Phases in Classical and Quantum Mechanics* (Springer)
- [44] Stobińska M et al 2019 Quantum interference enables constant-time quantum information processing *Sci. Adv.* **5** eaau9674

- [45] Banaszek K and Wódkiewicz K 1999 Testing quantum nonlocality in phase space *Phys. Rev. Lett.* **82** 2009
- [46] Wódkiewicz K 2000 Nonlocality of the Schrödinger cat *New J. Phys.* **2** 21
- [47] Kuzmich A, Walmsley I A and Mandel L 2001 Violation of a Bell-type inequality in the homodyne measurement of light in an Einstein-Podolsky-Rosen state *Phys. Rev. A* **64** 063804
- [48] Jeong H, Son W, Kim M S, Ahn D and Brukner Č 2003 Quantum nonlocality test for continuous-variable states with dichotomic observables *Phys. Rev. A* **67** 012106
- [49] Lee S-W and Jeong H 2011 High-dimensional Bell test for a continuous-variable state in phase space and its robustness to detection inefficiency *Phys. Rev. A* **83** 022103
- [50] Mycroft M E, McDermott T, Buraczewski A and Stobińska M 2023 Proposal for the distribution of multiphoton entanglement with optimal rate-distance scaling *Phys. Rev. A* **107** 012607
- [51] Sekatski P, Sangouard N, Stobińska M, Bussières F, Afzelius M and Gisin N 2012 Proposal for exploring macroscopic entanglement with a single photon and coherent states *Phys. Rev. A* **86** 060301
- [52] Paris M G A 1996 Displacement operator by beam splitter *Phys. Lett. A* **217** 78
- [53] Lvovsky A I and Raymer M G 2009 Continuous-variable optical quantum-state tomography *Rev. Mod. Phys.* **81** 299
- [54] Nielsen M A and Chuang I L 2010 *Quantum Computation and Quantum Information* (Cambridge University Press)
- [55] Summers S J and Werner R 1987 Maximal violation of Bell's inequalities is generic in quantum field theory *Commun. Math. Phys.* **110** 247
- [56] Gheorghiu A, Wallden P and Kashefi E 2017 Rigidity of quantum steering and one-sided device-independent verifiable quantum computation *New J. Phys.* **19** 023043
- [57] Dastidar M G and Sarbicki G 2022 Detecting entanglement between modes of light *Phys. Rev. A* **105** 062459
- [58] Fukuda D *et al* 2011 Titanium-based transition-edge photon number resolving detector with 98% detection efficiency with index-matched small-gap fiber coupling *Opt. Express* **19** 870–5
- [59] Lolli L, Taralli E and Rajteri M 2012 Ti/Au TES to discriminate single photons *J. Low Temp. Phys.* **167** 803–8
- [60] Stasi L, Caspar P, Brydges T, Zbinden H, Bussi eres F and Thew R 2023 High-efficiency photon-number-resolving detector for improving heralded single-photon sources *Quantum Sci. Technol.* **8** 045006
- [61] Stasi L, Gras G, Berrazouane R, Perrenoud M, Zbinden H and Bussieres F 2023 Fast high-efficiency photon-number-resolving parallel superconducting nanowire single-photon detector *Phys. Rev. Appl.* **19** 064041
- [62] Hu P, Li H, You L, Wang H, Xiao Y, Huang J, Yang X, Zhang W, Wang Z and Xie X 2020 Detecting single infrared photons toward optimal system detection efficiency *Opt. Express* **28** 36884–91
- [63] Chang J *et al* 2021 Detecting telecom single photons with 99.5 + 0.5 – 2.07% system detection efficiency and high time resolution *APL Photon.* **6** 2021
- [64] Zhu D, Colangelo M, Chen C, Korzh B A, Wong F N C, Shaw M D and Berggren K K 2020 Resolving photon numbers using a superconducting nanowire with impedance-matching taper *Nano Lett.* **20** 3858–63
- [65] Endo M, Sonoyama T, Matsuyama M, Okamoto F, Miki S, Yabuno M, China F, Terai H and Furusawa A 2021 Quantum detector tomography of a superconducting nanostrip photon-number-resolving detector *Opt. Express* **29** 11728–38
- [66] Clinton C, Nicolich K L, Islam N T, Lafyatis G P, Miller A J, Gauthier D J and Kim J 2017 Multi-photon detection using a conventional superconducting nanowire single-photon detector *Optica* **4** 1534–5
- [67] Cheng R, Zhou Y, Wang S, Shen M, Taher T and Tang H X 2023 A 100-pixel photon-number-resolving detector unveiling photon statistics *Nat. Photon.* **17** 112–9
- [68] Eberhard P H 1993 Background level and counter efficiencies required for a loophole-free Einstein-Podolsky-Rosen experiment *Phys. Rev. A* **47** R747(R)